AD-A149 425 STRESS CONCENTRATION DUE TO AXIAL TENSION OF LOADED NONSYMMETRIC-SHAPED G.. (U) ARMY ARMAMENT RESEARCH AND DEVELOPMENT CENTER WATERVLIET NY L.. Y F CHENG NOV 84 1/1

UNCLASSIFIED ARLCB-TR-84037 SBI-AD-E440 266 F/G 20/11 NL

END

FILMED

DTIC

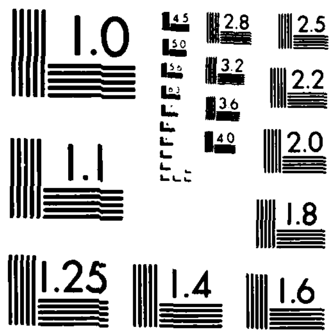

MICROCOPY RESOLUTION TEST CHART
NATIONAL BUREAU OF STANDARDS-1963-A

AD-A149 425

(12)

AD E440 266

TECHNICAL REPORT ARLCB-TR-84037

STRESS CONCENTRATION DUE TO AXIAL TENSION OF LOADED NONSYMMETRIC-SHAPED GROOVES

Y. F. CHENG

NOVEMBER 1984

US ARMY ARMAMENT RESEARCH AND DEVELOPMENT CENTER
LARGE CALIBER WEAPON SYSTEMS LABORATORY
BENÉT WEAPONS LABORATORY
WATERVLIET N.Y. 12189

DISCLAIMER

The findings in this report are not to be construed as an official Department of the Army position unless so designated by other authorized documents.

The use of trade name(s) and/or manufacture(s) does not constitute an official indorsement or approval.

DISPOSITION

Destroy this report when it is no longer needed. Do not return it to the originator.

SECURITY CLASSIFICATION OF THIS PAGE (When Data Entered)

REPORT DOCUMENTATION PAGE

READ INSTRUCTIONS BEFORE COMPLETING FORM

1. REPORT NUMBER: ARLCB-TR-84037	2. GOVT ACCESSION NO.: AD A149425	3. RECIPIENT'S CATALOG NUMBER
4. TITLE (and Subtitle): STRESS CONCENTRATION DUE TO AXIAL TENSION OF LOADED NONSYMMETRIC-SHAPED GROOVES		5. TYPE OF REPORT & PERIOD COVERED: Final
		6. PERFORMING ORG. REPORT NUMBER
7. AUTHOR(s): Y. F. Cheng		8. CONTRACT OR GRANT NUMBER(s)
9. PERFORMING ORGANIZATION NAME AND ADDRESS: US Army Armament Research & Development Center, Benet Weapons Laboratory, SMCAR-LCB-TL, Watervliet, NY 12189		10. PROGRAM ELEMENT, PROJECT, TASK AREA & WORK UNIT NUMBERS: AMCMS No. 6111.02.H600.011, PRON No. 1A425M541A1A
11. CONTROLLING OFFICE NAME AND ADDRESS: US Army Armament Research & Development Center, Large Caliber Weapon Systems Laboratory, Dover, NJ 07801		12. REPORT DATE: November 1984
		13. NUMBER OF PAGES
14. MONITORING AGENCY NAME & ADDRESS (if different from Controlling Office)		15. SECURITY (of this report): UNCLASSIFIED
		15a. DECLASSIFICATION/DOWNGRADING SCHEDULE

16. DISTRIBUTION STATEMENT (of this Report)

Approved for public release; distribution unlimited.

17. DISTRIBUTION STATEMENT (of the abstract entered in Block 20, if different from Report)

18. SUPPLEMENTARY NOTES

Presented at Fifth International Congress on Experimental Mechanics, Montreal, Canada, 10-15 June 1984.
Published in proceedings of the congress.

19. KEY WORDS (Continue on reverse side if necessary and identify by block number)

Lug and Groove Connection
Stress Concentration
Nonsymmetric-Shaped Grooves
Two-Dimensional Photoelasticity
Heywood's Equation

20. ABSTRACT (Continue on reverse side if necessary and identify by block number)

Lug and groove connections are frequently found in structures where two components meet and loads are transmitted. These grooves usually have a nonsymmetric shape, i.e., the flank angle at the loaded face is different from that at the free face. While numerous data on stress concentrations for symmetric-shaped grooves (for example, U- or V-shaped) are available, very little information exists for nonsymmetric-shaped grooves. This report

(CONT'D ON REVERSE)

20. ABSTRACT (CONT'D)

describes a photoelastic study on stress concentration in plates due to axial tension of loaded nonsymmetric-shaped grooves. Groove geometries as well as loading conditions are given. Maximum groove stresses were found and stress concentration factors were calculated. Also, parametric curves of stress concentration were obtained. A comparison was made between experimental results and those calculated by means of Heywood's equation.

TABLE OF CONTENTS

	Page
ACKNOWLEDGEMENT	iii
INTRODUCTION	1
MODELS AND LOADING	1
APPARATUS AND EXPERIMENTAL TECHNIQUES	5
RESULTS AND DISCUSSION	6
Remote Loading	6
Distributed Flank Loading	9
Concentrated Flank Loading	10
Loaded Projection	16
Heywood's Empirical Equation	17
CONCLUSIONS	20
REFERENCES	23

TABLES

I.	MODEL THICKNESS AND GROOVE RADIUS	3
II.	STRESS CONCENTRATION FACTOR K FOR NONSYMMETRIC-SHAPED GROOVES UNDER REMOTE TENSION, d/D = 0.7	6
III.	STRESS CONCENTRATION FACTOR K FOR NONSYMMETRIC-SHAPED GROOVES UNDER DISTRIBUTED FLANK LOADING d/D = 0.7	9
IV.	STRESS CONCENTRATION FACTOR K FOR NONSYMMETRIC-SHAPED GROOVES UNDER CONCENTRATED FLANK LOADING, d/D = 0.7	14
V.	STRESS CONCENTRATION FACTOR K IN CONCENTRATEDLY LOADED PROJECTIONS	16
VI.	COMPARISON BETWEEN STRESS CONCENTRATION FACTOR OBTAINED EXPERIMENTALLY AND FROM HEYWOOD'S EQUATION	20

Page

LIST OF ILLUSTRATIONS

1. Sketch of models. 2

2. Sketch of flank loading fixture. 4

3. Boundary fringe distribution of nonsymmetric-shaped grooves under remote tension. R = t = 6.35 mm, W = 267 Newton, Model material: PSM-1. 7

4. Stress concentration factor K versus R/d in plates with nonsymmetric-shaped grooves under remote tension, d/D = 0.7. 8

5. Stress concentration factor K versus R/d in plates with nonsymmetric-shaped grooves under distributed flank loading. 11

6. Stress concentration factor K versus $2\ell\cos 7°/(D-d)$ in plates with nonsymmetric-shaped grooves under distributed flank loading. 12

7. Stress concentration factor K versus R/d in plates with nonsymmetric-shaped grooves under concentrated flank loading. 13

8. Stress concentration factor K versus 2L/(D-d) in plates with nonsymmetric-shaped grooves under concentrated flank loading. 15

9. Stress concentration factor K versus 2L/(D-d) in loaded projections. 18

10. Dimensions used for calculating maximum groove stress by Heywood. 19

11. Comparison between stress concentration factors obtained experimentally and from Heywood's equation. 21

ACKNOWLEDGEMENT

Charles Cobb's participation in the experimental phase of this investigation is hereby acknowledged.

INTRODUCTION

Lug and groove connections are frequently found in structures where two components meet and loads are transmitted. These grooves usually have a nonsymmetric shape, i.e., the flank angle at the loaded face is different from that at the free face. While numerous data on stress concentrations for symmetric-shaped grooves (for example, U- or V-shaped) are available (ref 1), very little information exists for nonsymmetric-shaped grooves. This report describes a photoelastic study on stress concentration in plates due to axial tension of loaded nonsymmetric-shaped grooves. Three loading conditions were investigated: remote load, concentrated flank load, and distributed flank load. The objectives were (1) to find how the magnitude and position of the maximum groove stresses vary with the groove geometry, the type of load, and the point of application of the load, and (2) to construct parametric curves of stress concentration factors for design use. In addition, the models were modified to resemble loaded projections and tested under concentrated flank load. The results were compared with those calculated by means of Heywood's equation (ref 2).

MODELS AND LOADING

Figures 1(a), (b), and (c) show sketches of models for investigations in remote load, flank load, and loaded projections, respectively. The grooves had a British standard buttress profile with a primary flank angle α of 7

---

[1]Peterson, R. E., Stress Concentration Factors, John Wiley & Sons, 1974.
[2]Heywood, R. B., "Tensile Stresses in Loaded Projections," Proceedings of the Institute of Mechanical Engineers, Vol. 159, pp. 384-391, 1948.

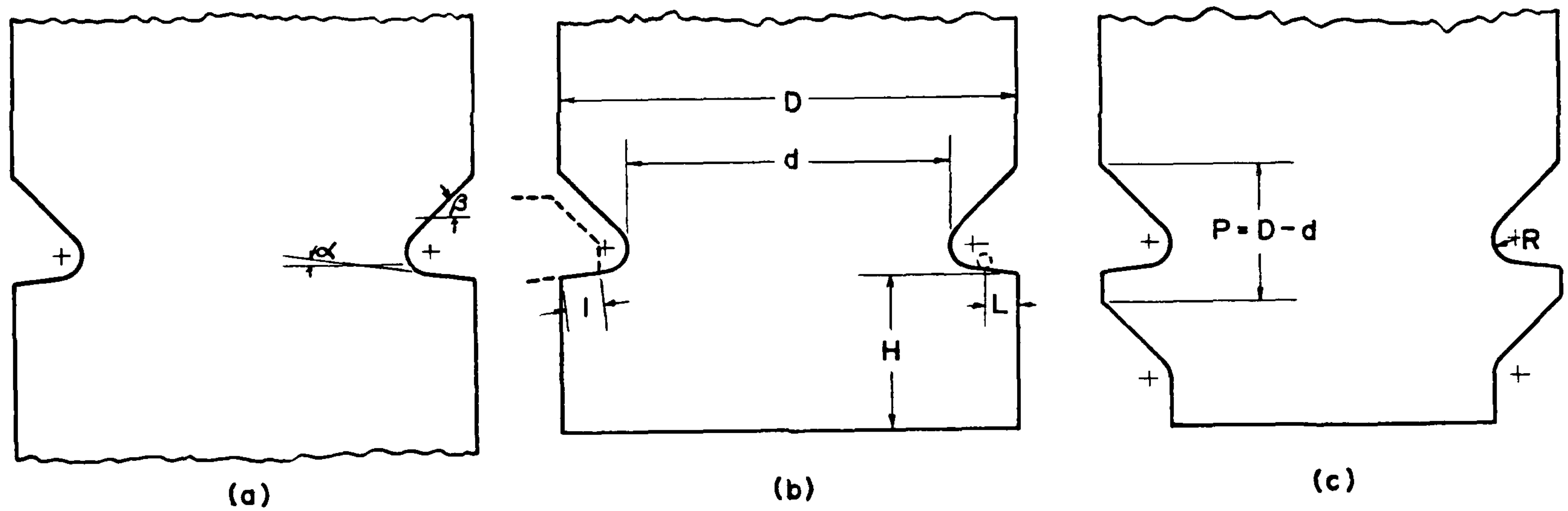

Fig. I   Sketch of models

degrees at the loaded face and a secondary flank angle β of 45 degrees. The models had a gross width D of 90 mm and a net width d of 63 mm at the narrowest transverse section. They were made of photoelastic model material type PSM-1, supplied by Measurement Group, Raleigh, NC. The material had a fringe value of 252 kPa per fringe per inch. Four combinations of model thickness and groove radius were studied. They are shown in Table I.

TABLE I. MODEL THICKNESS AND GROOVE RADIUS

Model	A	B	C	D
Thickness, t, mm	3.18	6.35	6.35	6.35
Radius, R, mm	3.18	6.35	9.53	12.7

Remote loads were applied through pins at both ends of the model, Figure 1(a). After tests in remote load were completed, the lower end containing primary flank was shortened and models for flank load with H = 0.5d were obtained, Figure 1(b). An aluminum fixture having two mating 7 degree inclined faces, Figure 2, was used to apply distributed loads to both flanks. Concentrated loads were applied via 3.2 mm diameter steel pins as shown by dotted lines in the figure. The length, ℓ, Figure 1(b), of loaded face in distributed load varied from 2.18 mm to 10.2 mm. The transverse distance L, Figure 1(b), from the edge of the model to the point of application of concentrated load varied from 2.34 mm to 10.7 mm. These results are shown in Tables III and IV in the following section.

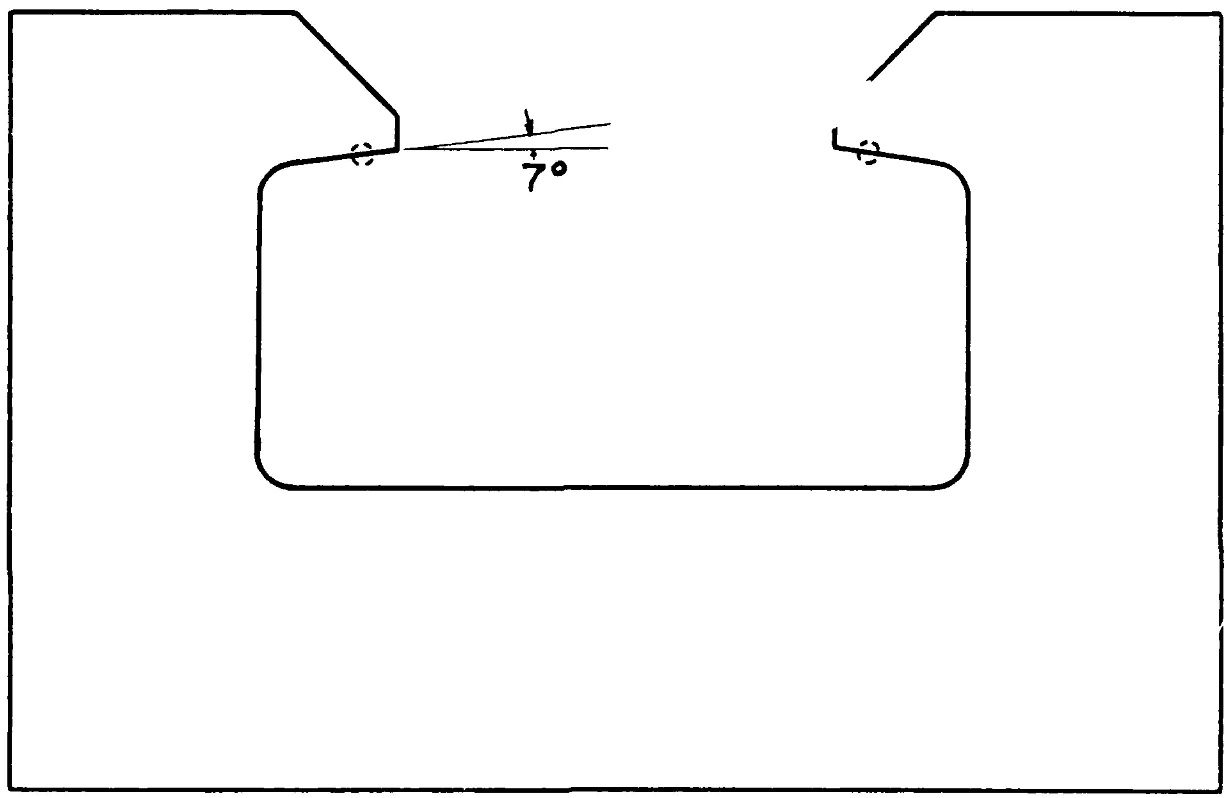

Fig. 2 Sketch of flank loading fixture

After tests in the flank load were completed, the models were again modified to resemble loaded projections, Figure 1(c). Model and loading geometries for this series of tests are shown in Table V in the following section.

All loads were applied in steps by means of a dead weight loading machine. Precautions were taken to ensure symmetry of loading. Also, maximum groove stress was kept within linear range of the model material.

APPARATUS AND EXPERIMENTAL TECHNIQUES

A lens-type transmission polariscope with collimated monochromatic light of 5461 Å was used. Photographs of isochromatic fringe patterns were taken in both bright and dark field after each step of loading. Maximum fringe order and its position were determined from 7-magnification of photographs.

On the free boundary one of the principal stresses was identically zero and the remaining principal stress tangent to the boundary was directly given by the fringe order. Stress concentration factor, K, was defined as the ratio of the maximum groove stress, σ_{max}, to the nominal stress, σ_{nom}, at the narrowest section. Thus

$$K = \sigma_{max}/\sigma_{nom} = (d)(t)(\sigma_{max})/W \quad (1)$$

where W is the load. Using the difference method, Eq. (1) was rewritten as

$$K = (d)(t)(\Delta\sigma_{max})/(\Delta W) \quad (2)$$

where Δ denotes increments between steps. Equation (2) was used to calculate K throughout this investigation.

RESULTS AND DISCUSSION

Remote Loading

Figure 3 shows a typical boundary fringe distribution of nonsymmetric-shaped grooves under remote tensile load. It can be seen that the maximum fringe order, hence, the maximum groove stress, σ_{max}, does not occur at the narrowest section. It is displaced toward the 7 degree face. Angular displacement varies from 1 degree for R/d = 0.2 to 5 degrees for R/d = 0.05. Results are shown in Table II and Figure 4. Stress concentration factor for U-grooves, K_u, is included for comparison (ref 1).

TABLE II. STRESS CONCENTRATION FACTOR K FOR NONSYMMETRIC-SHAPED GROOVES UNDER REMOTE TENSION, d/D = 0.7

Test	R/d	K	Angular Displacement, Degrees	K_u	Reduction, $\frac{K_u-K}{K_u} \times 100\%$
A	0.05	3.25	5.0	3.47	6.34
B	0.10	2.75	3.2	2.87	4.18
C	0.15	2.38	2.0	2.43	2.05
D	0.20	2.15	1.0	2.18	1.37

It is known that most materials in straight sides of U-grooves are idle and do not carry any load. In comparison with U-grooves, materials in nonsymmetric-shaped grooves are better utilized, stresses are redistributed, and maximum groove stress and stress concentration are reduced. The degree of reduction, based on K_u, varies from 1.4 percent for R/d = 0.20 to 6.3 percent

---

[1]Peterson, R. E., Stress Concentration Factors, John Wiley & Sons, 1974.

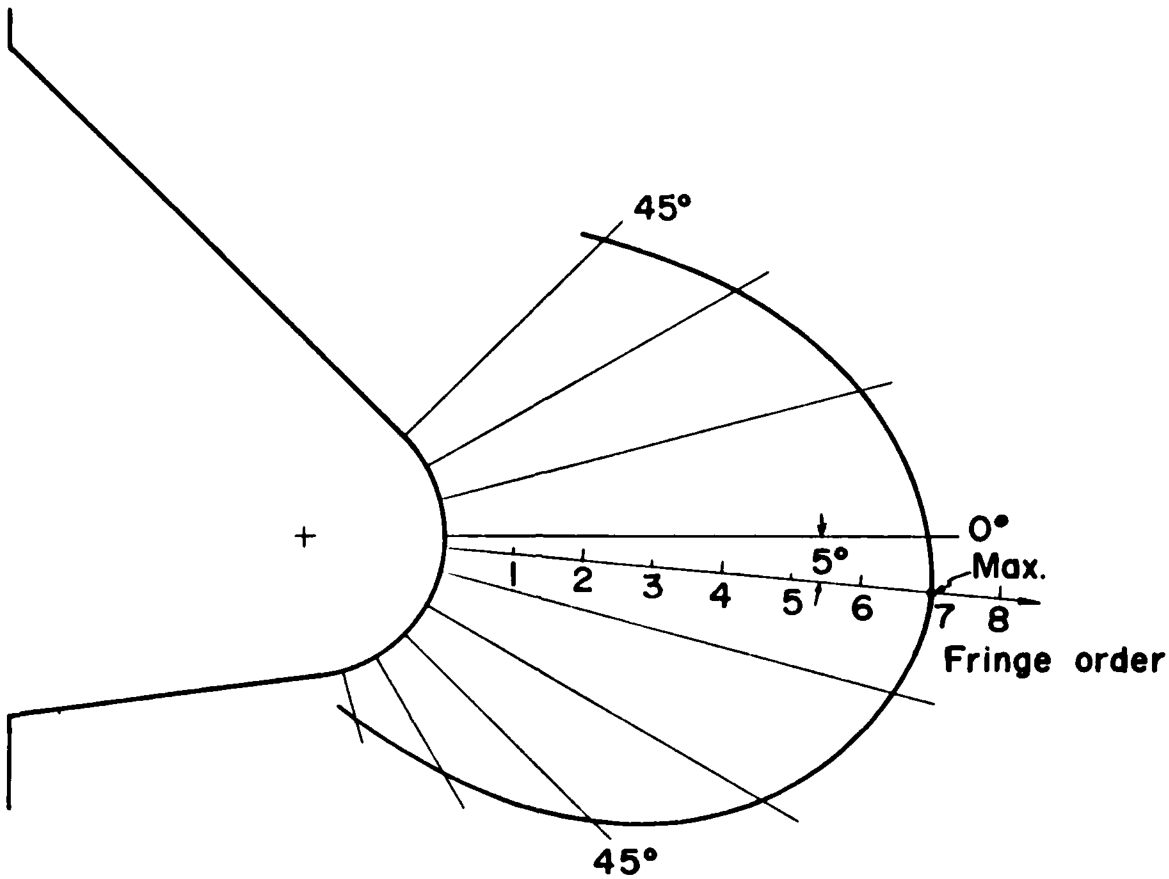

Fig. 3 Boundary fringe distribution of nonsymmetric-shaped grooves under remote tension
R=t=6.35mm, W=267 newton, Material: PSM-1

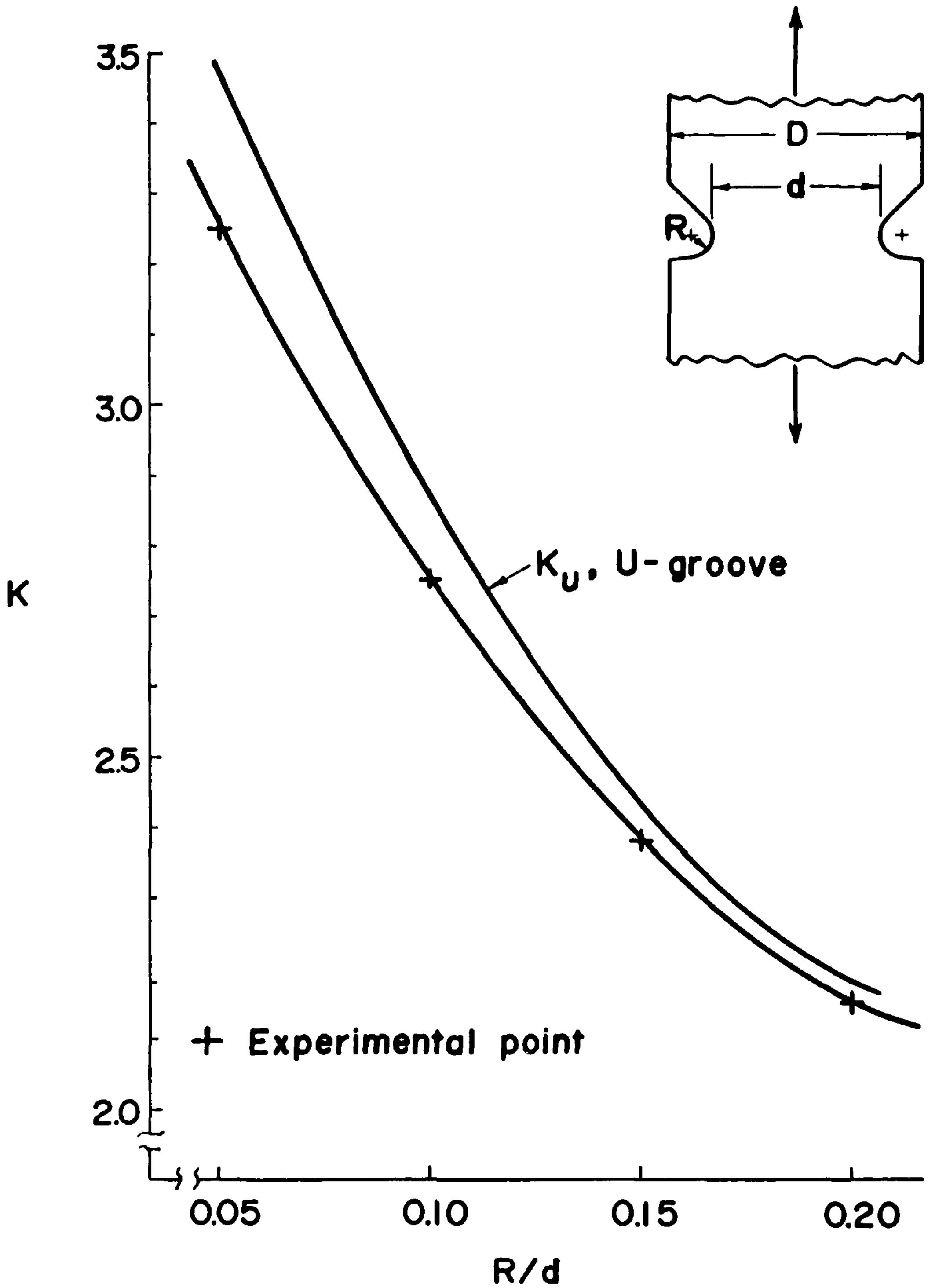

Fig. 4 Stress concentration factor K versus R/d in plates with nonsymmetric-shaped grooves under remote tension, d/D = 0.7

for R/D = 0.05.

Distributed Flank Loading

Table III shows that the angular displacement in distributed flank loading has a larger value than that under remote loading. The maximum groove stress is displaced farther toward the 7 degree loaded face. Angular displacement varies directly with groove radius R and inversely with the length of loaded face ℓ.

TABLE III. STRESS CONCENTRATION FACTOR K FOR NONSYMMETRIC-SHAPED GROOVES UNDER DISTRIBUTED FLANK LOADING, d/D = 0.7

Test	R/d	ℓ, mm	K	Angular Displacement, Degree	$2\ell\cos 7°/(D-d)$
A11	0.05	10.2	8.01	30.0	0.76
A12	0.05	7.01	8.55	35.0	0.52
A13	0.05	4.98	8.81	38.0	0.37
A14	0.05	2.18	8.60	40.0	0.16
B11	0.10	7.01	6.43	37.5	0.52
B12	0.10	4.98	7.33	39.0	0.37
B13	0.10	2.18	6.97	43.0	0.16
C11	0.15	4.98	5.77	40.0	0.37
C12	0.15	2.18	6.33	46.0	0.16
D11	0.20	2.18	6.23	75.0	0.16

Figure 5 shows values of K versus R/d. Stress concentration under remote tension was included. A curve was drawn passing through points of $\ell = 2.18$ mm. The results indicate that (1) K varies inversely with groove radius R, and (2) under distributed flank load K is about 2.5 to 3 times as high as that under remote tension.

Figure 6 shows values of K versus $2\ell\cos 7°/(D-d)$, a ratio of transverse projection of the length of loaded face, $\ell\cos 7°$, to the groove depth, $(D-d)/2$. A curve was drawn through points of $R/d = 0.05$. The results indicate that, at least for values of $R/d \leq 0.1$, K increases as the length of loading ℓ is reduced, reaches a maximum at approximately $2\ell\cos 7°/(D-d) = 0.3$, and then starts to decrease as ℓ is further reduced.

Concentrated Flank Loading

The tests made under concentrated flank loading and their results are shown in Table IV. Within the ranges of geometries and load points, the angular displacement of maximum groove stress varies from 22.5 degrees to 38.5 degrees, considerably less than that under distributed flank loading. Same as under distributed loading, the angular displacement varies directly with groove radius R and inversely with the distance L.

Figure 7 shows that K decreases as groove radius R is increased. It also shows that under concentrated flank loading K is considerably higher than that under remote tension. A comparison between Figures 5 and 7 reveals that, in general, for small values of R, K is higher under concentrated flank load than that under distributed flank load, and conversely for larger values of R.

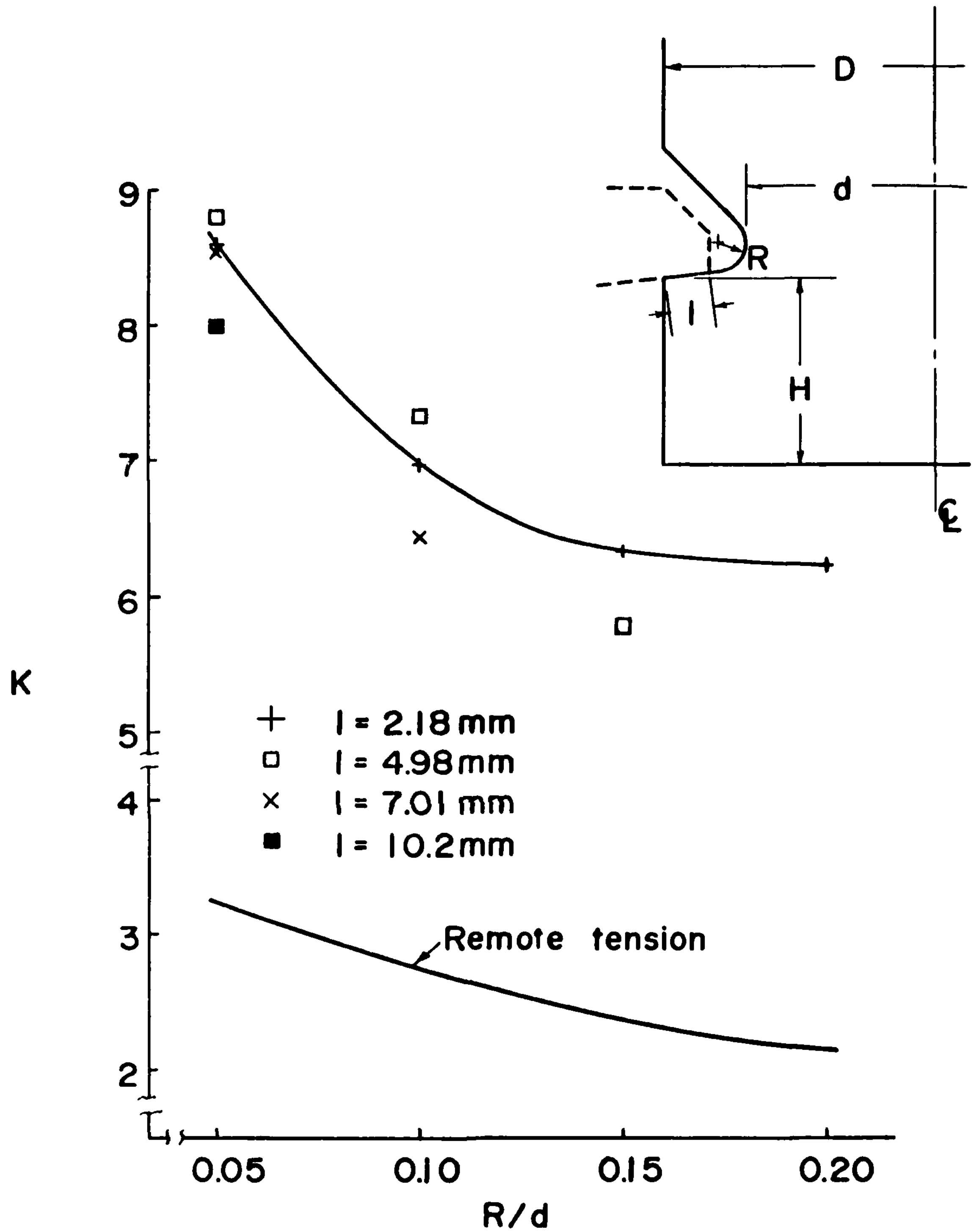

Fig. 5 Stress concentration factor K versus R/d in plates with nonsymmetric-shaped grooves under distributed flank loading

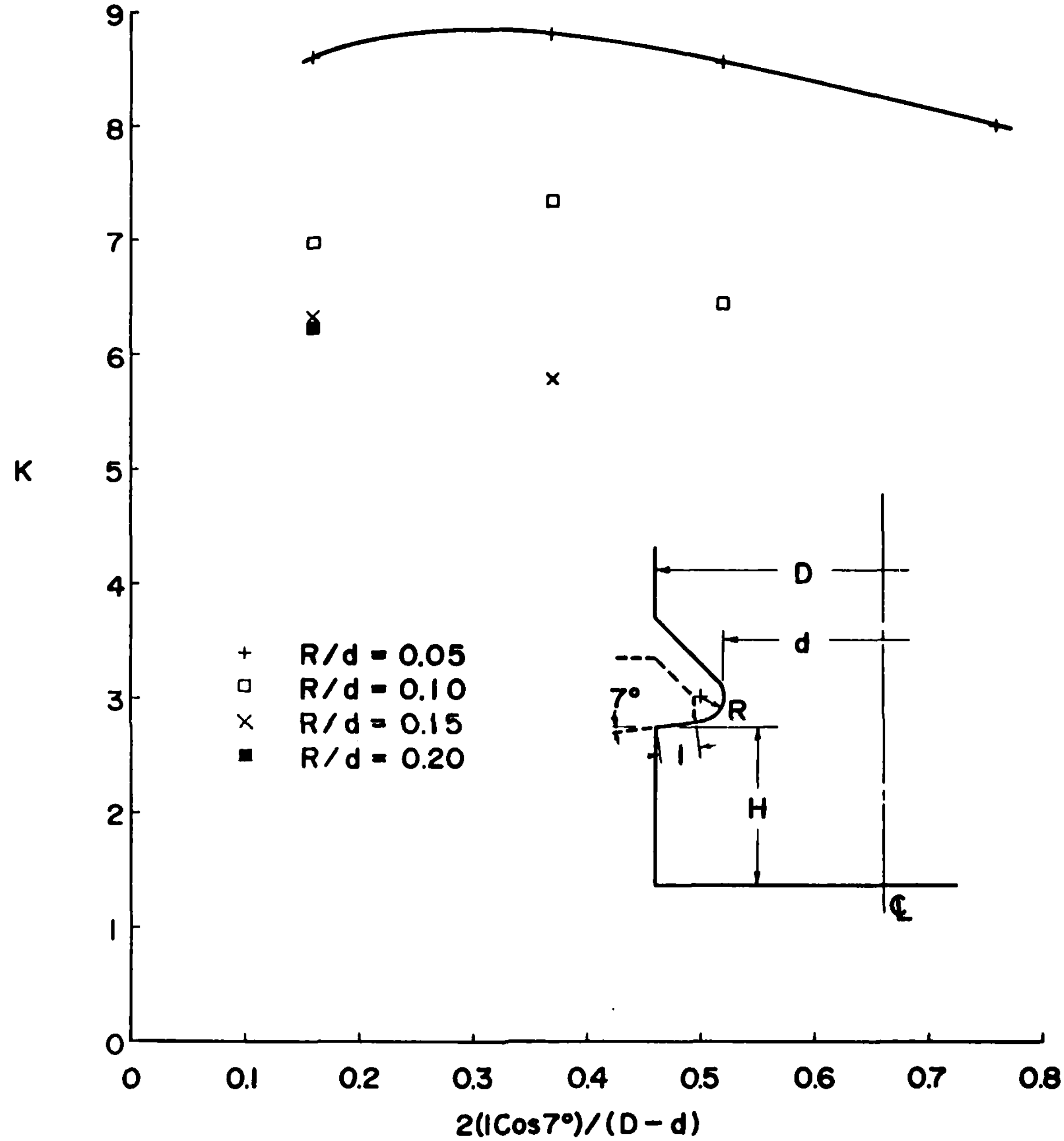

Fig. 6 Stress concentration factor K versus 2(lCos7°)/(D − d) in plates with nonsymmetric-shaped grooves under distributed flank loading

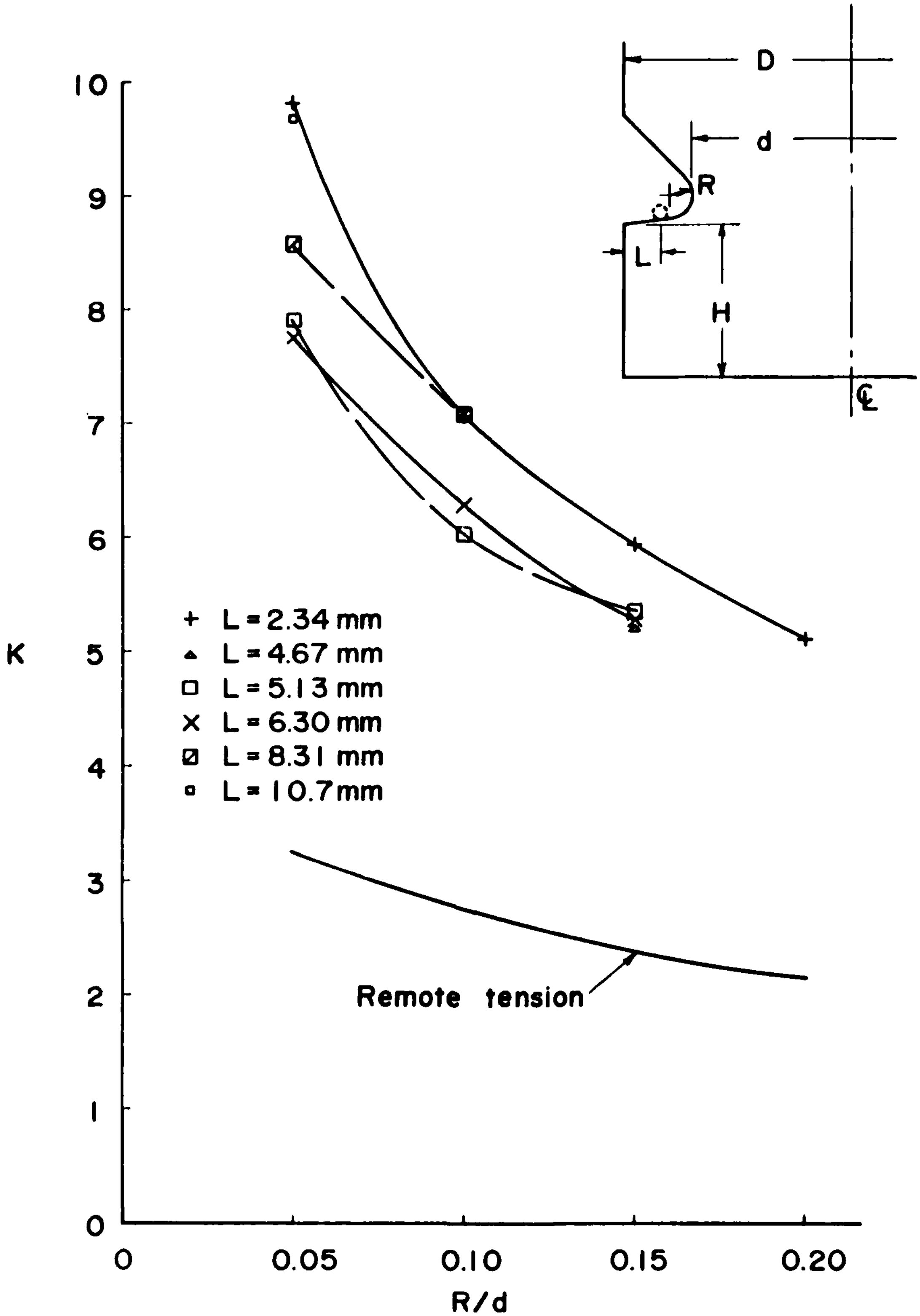

Fig. 7 Stress concentration factor K versus R/d in plates with nonsymmetric-shaped grooves under concentrated flank loading

TABLE IV. STRESS CONCENTRATION FACTOR K FOR NONSYMMETRIC-SHAPED GROOVES UNDER CONCENTRATED FLANK LOADING, d/D = 0.7

Test	R/d	L, mm	K	Angular Displacement, Degrees	2L/(D-d)
A21	0.05	10.7	9.67	22.5	0.80
A22	0.05	8.31	8.57	22.0	0.62
A23	0.05	6.30	7.75	30.0	0.47
A24	0.05	5.13	7.89	30.0	0.39
A25	0.05	2.34	9.81	34.5	0.18
B21	0.10	8.31	7.07	35.0	0.62
B22	0.10	6.30	6.28	31.5	0.47
B23	0.10	5.13	6.02	35.0	0.39
B24	0.10	2.34	7.05	36.5	0.18
C21	0.15	6.30	5.27	30.0	0.47
C22	0.15	5.13	5.34	33.0	0.39
C23	0.15	4.67	5.21	37.5	0.35
C24	0.15	2.34	5.93	38.5	0.18
D21	0.20	2.34	5.11	38.0	0.18

Figure 8 shows values of K versus 2L/(D-d), a ratio of transverse direction, L, to the groove depth (D-d)/2. The results indicate that K decreases as the load is moved out from the groove, reaches a minimum, and then starts to increase as the load is moved out farther.

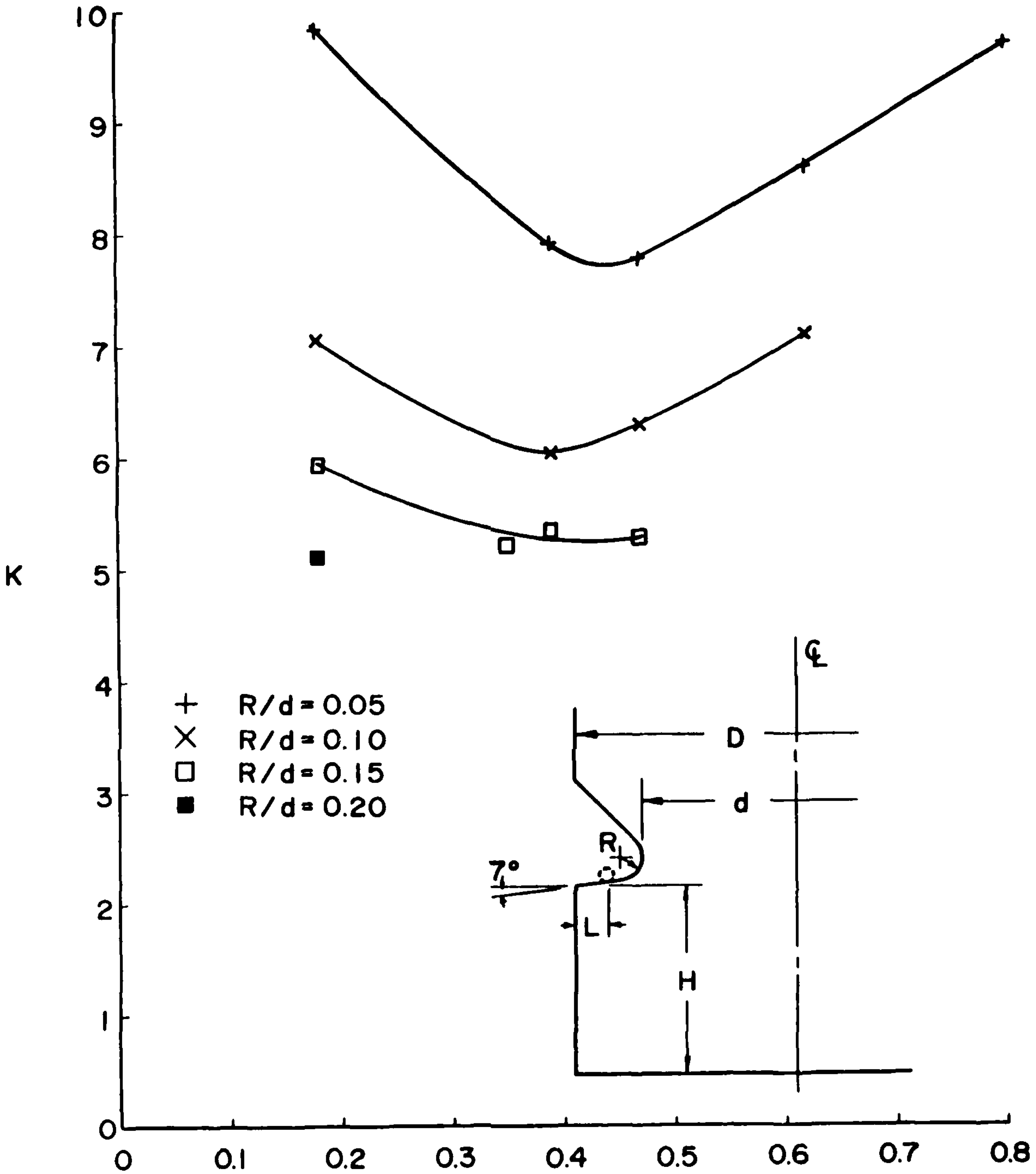

Fig. 8 Stress concentration factor K versus 2L/(D−d) in plates with nonsymmetric-shaped grooves under concentrated flank loading

A comparison between Figures 6 and 8 further reveals that K reaches a maximum between extremes of ℓ under distributed load, but a minimum between extremes of L under concentrated load.

Loaded Projection

It can be seen in Table V that the angular displacement of maximum groove stress has the same trend found in flank loading, i.e., it varies directly with R and inversely with L. However, the displaced magnitude is larger in loaded projection than that in concentrated flank loading.

TABLE V. STRESS CONCENTRATION FACTOR K IN CONCENTRATEDLY LOADED PROJECTIONS

Test	R/d	L, mm	K	Angular Displacement, Degrees	2L/(D-d)
A31	0.05	10.7	10.9	26.0	0.80
A32	0.05	8.31	9.17	26.0	0.62
A33	0.05	6.30	9.55	29.0	0.47
A34	0.05	5.13	10.5	32.5	0.39
A35	0.05	2.34	11.9	38.0	0.18
B31	0.10	8.31	7.05	37.0	0.62
B32	0.10	6.30	6.63	37.0	0.47
B33	0.10	5.13	6.90	38.0	0.39
B34	0.10	2.34	8.40	50.0	0.18

Figure 9 shows curves of K versus 2L/(D-d). Results from concentrated flank load are included for comparison. It can be seen that stress concentrations under loaded projection are higher than those under concentrated flank loading. Moreover, K has the same trend found in concentrated flank loading, i.e., it decreases as the load is moved away from the groove, reaches a minimum, and then starts to increase as the load is moved farther away.

Heywood's Empirical Equation

In 1948, Heywood (ref 2) suggested an empirical equation of the following form:

$$\sigma_{max} = [1 + 0.26(e/R)^{0.7}][(1.5\ a/e^2) + (0.36/be)^{1/2}(1+0.25\sin\gamma)](W/t) \quad (3)$$

for calculating the maximum groove stress σ_{max} in loaded projection, Figure 10. In this equation, it was assumed that σ_{max} falls at point A, 30 degrees from the point of tangency on the groove, and the dimensions a, b, and e, and the angle γ are as shown in the figure. Recently, Allison and Hearn (ref 3) reported the movement of maximum groove stress position in a range of angle from 30 degrees to 70 degrees as load point is varied. Our results shown in this report as well as previous results (ref 4) are well within this range.

Following Eq. (3), stress concentration factor can be expressed as

$$(\sigma_f)_{max}\cdot d/(2W/t) = [1+0.26(e/R)^{0.7}][(1.5a/e^2) + (0.36/be)^{1/2}(1+0.25\sin\gamma)](d/2) \quad (4)$$

---

[2]Heywood, R. B., "Tensile Stresses in Loaded Projections," Proceedings of the Institute of Mechanical Engineers, Vol. 159, 1948, pp. 384-391.

[3]Allison, I. M. and Hearn, E. J., "A New Look at the Bending Strength of Gear Teeth," Experimental Mechanics, V. 20, No. 7, July 1980, pp. 217-225.

[4]Cheng, Y. F., "A Photoelastic Investigation of Stresses and Load Distributions in Lug-Groove Joints," Proceedings of the Army Symposium on Solid Mechanics, 1982, pp. 454-470.

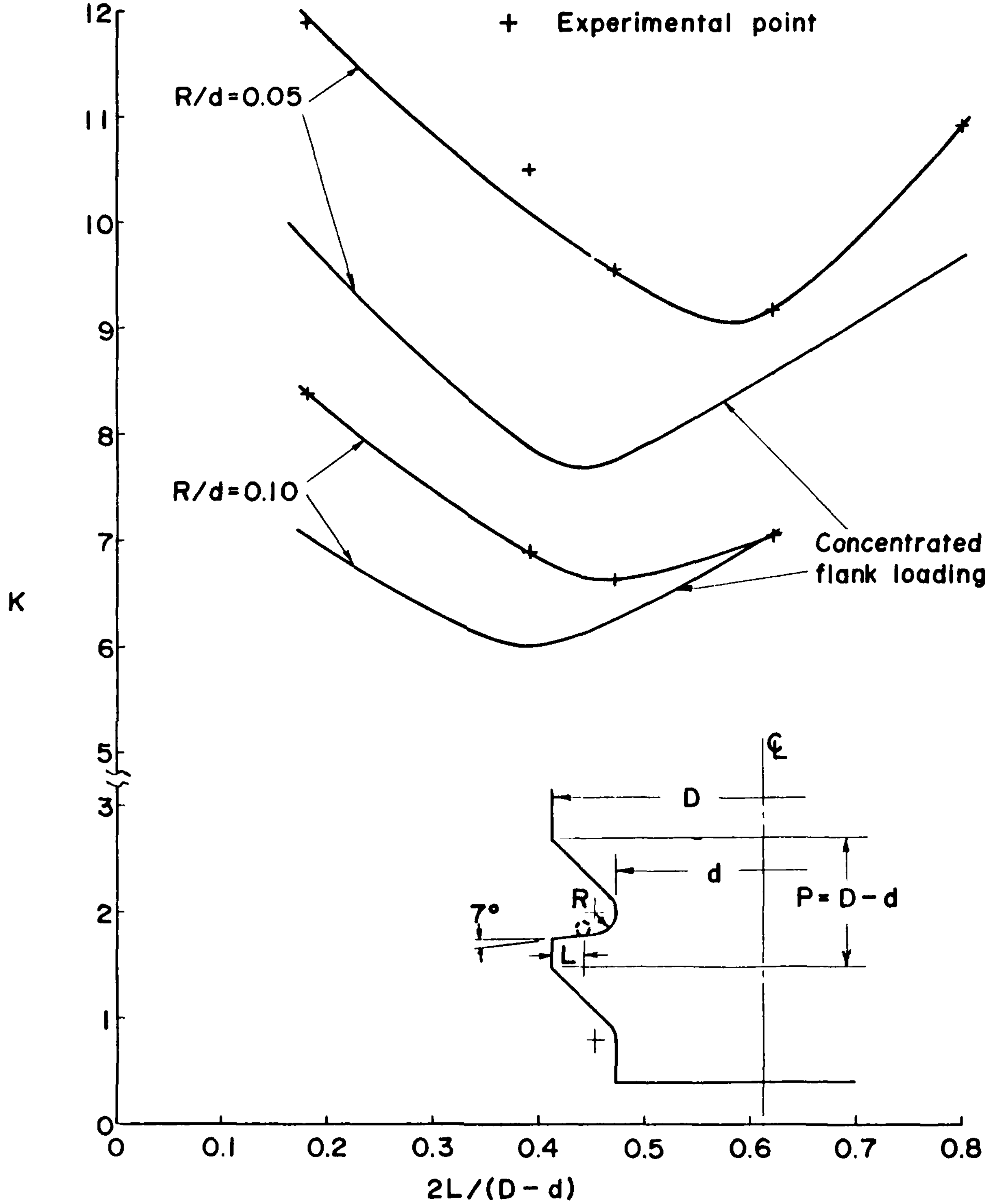

Fig. 9 Stress concentration factor K versus 2L/(D−d) in loaded projections

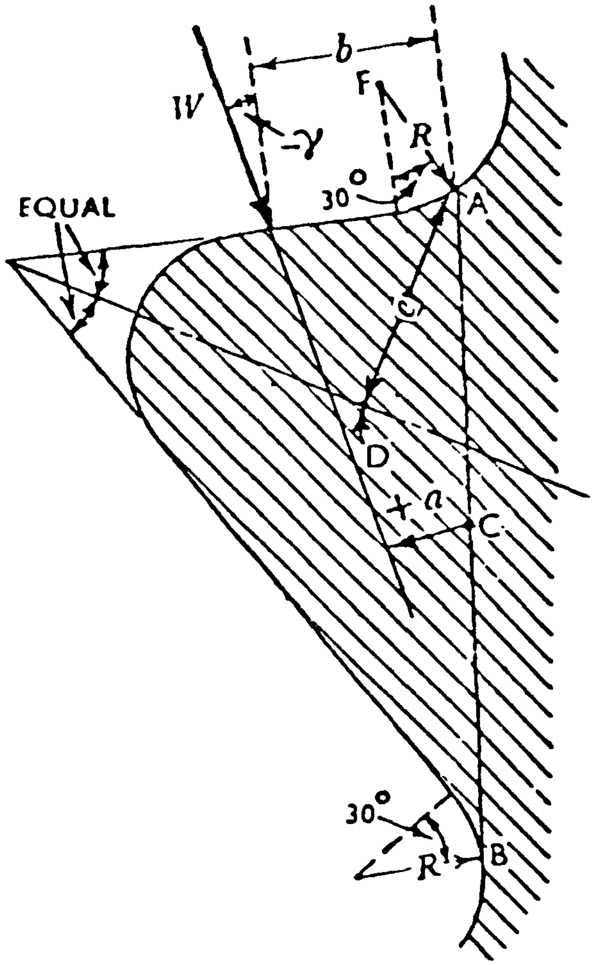

Fig. 10. Dimensions used for calculating maximum groove stress by Heywood.

They were calculated for tests A31-A35 and B31-B34 and shown in Table VI.

TABLE VI. COMPARISON BETWEEN STRESS CONCENTRATION FACTOR OBTAINED EXPERIMENTALLY AND FROM HEYWOOD'S EQUATION

Test	R, mm	L, mm	K	$(\sigma_f)_{max} \cdot d/(2W/t)$
A31	3.18	10.7	10.9	10.0
A32	3.18	8.31	9.17	9.38
A33	3.18	6.30	9.55	10.4
A34	3.18	5.13	10.5	11.2
A35	3.18	2.34	11.9	13.3
B31	6.35	8.31	7.05	8.59
B32	6.35	6.30	6.63	9.06
B33	6.35	5.13	6.90	9.65
B34	6.35	2.34	8.40	11.4

It can be seen from Table VI and Figure 11 that Heywood's values are high. Perhaps this equation is not applicable to lug-groove or screw-thread connections since sectional dimensions are not included.

CONCLUSIONS

The following conclusions are made for stress concentration in plates due to axial tension of loaded nonsymmetric-shaped grooves.

1. Stress concentration factor K varies inversely with groove radius R under all loading conditions (remote tension, distributed flank load, concentrated flank load, and loaded projections).

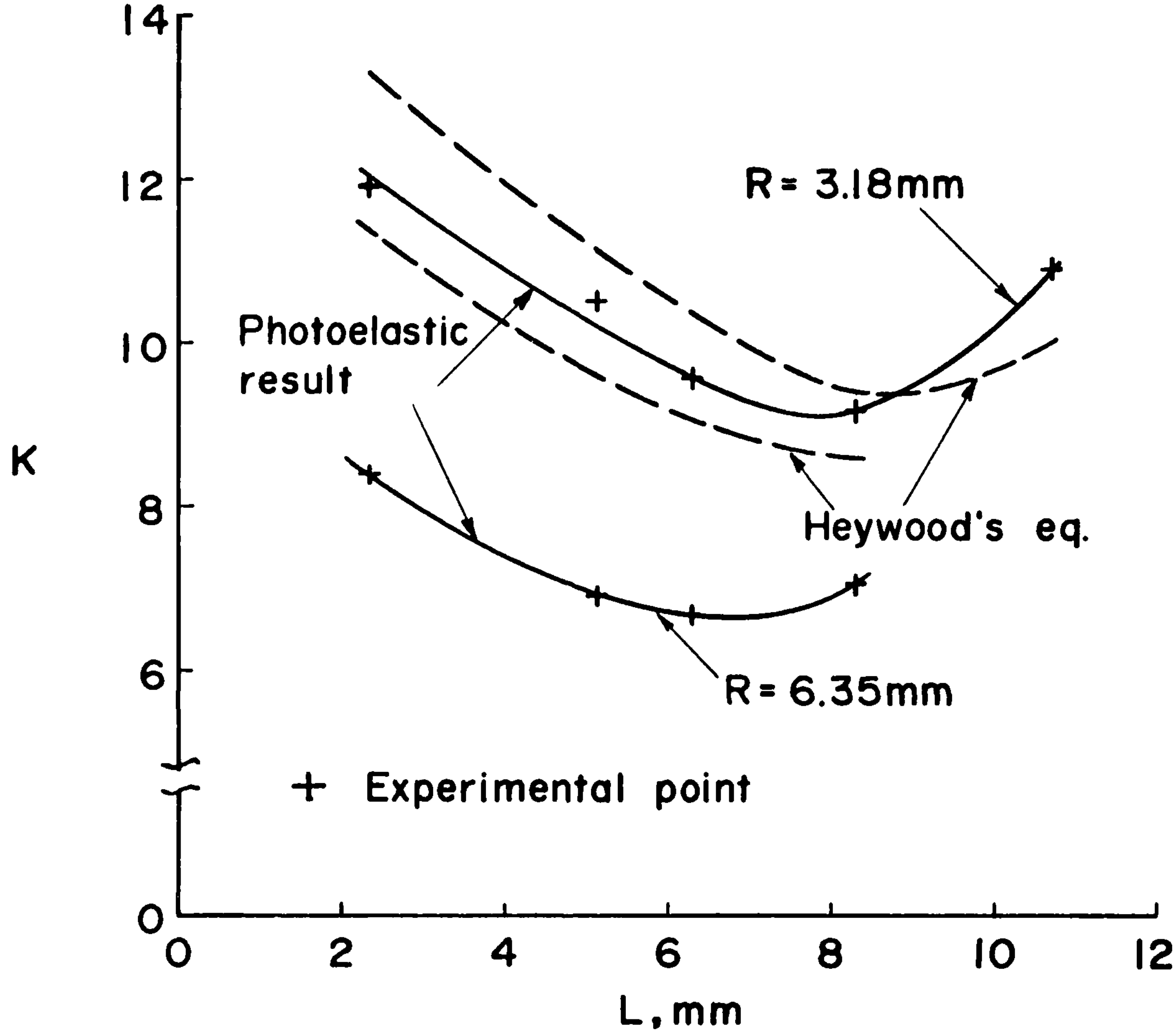

Fig. 11 Comparison between stress concentration factors obtained experimentally and from Heywood's equation

2. Stress concentration factor K in loaded projections is higher than that in concentrated flank load.

3. Stress concentration factor K in flank load (distributed and concentrated) is higher than that in remote tension.

4. For shorter groove radius, K is higher under concentrated flank load than under distributed flank load, and conversely for longer groove radius.

5. K has a maximum between extremes of ℓ under distributed flank load, but a minimum between extremes of L under concentrated flank load and loaded projections.

6. The position of maximum groove stress is displaced toward the loaded flank under all flank loading (distributed, concentrated, and loaded projections) and is displaced toward the flank with small flank angle under remote tension. In general, angular displacement varies directly with R and inversely with ℓ or L.

7. Heywood's values are high. Perhaps, Heywood's equation should not be applied in lug-groove or screw-thread connections since sectional dimensions are not included.

8. Under remote tension, a nonsymmetric-shaped groove has lower stress concentration than a symmetric-shaped U-groove.

REFERENCES

1. Peterson, R. E., Stress Concentration Factors, John Wiley & Sons, 1974.

2. Heywood, R. B., "Tensile Stresses in Loaded Projections," Proceedings of the Institute of Mechanical Engineers, Vol. 159, 1948, pp. 384-391.

3. Allison, I. M. and Hearn, E. J., "A New Look at the Bending Strength of Gear Teeth," Experimental Mechanics, V. 20, No. 7, July 1980, pp. 217-225.

4. Cheng, Y. F., "A Photoelastic Investigation of Stresses and Load Distributions in Lug-Groove Joints," Proceedings of the Army Symposium on Solid Mechanics, 1982, pp. 454-470.

TECHNICAL REPORT INTERNAL DISTRIBUTION LIST

	NO. OF COPIES
CHIEF, DEVELOPMENT ENGINEERING BRANCH	
ATTN: SMCAR-LCB-D	1
-DA	1
-DP	1
-DR	1
-DS (SYSTEMS)	1
-DS (ICAS GROUP)	1
-DC	1
CHIEF, ENGINEERING SUPPORT BRANCH	
ATTN: SMCAR-LCB-S	1
-SE	1
CHIEF, RESEARCH BRANCH	
ATTN: SMCAR-LCB-R	2
-R (ELLEN FOGARTY)	1
-RA	1
-RM	2
-RP	1
-RT	1
TECHNICAL LIBRARY ATTN: SMCAR-LCB-TL	5
TECHNICAL PUBLICATIONS & EDITING UNIT ATTN: SMCAR-LCB-TL	2
DIRECTOR, OPERATIONS DIRECTORATE	1
DIRECTOR, PROCUREMENT DIRECTORATE	1
DIRECTOR, PRODUCT ASSURANCE DIRECTORATE	1

NOTE: PLEASE NOTIFY DIRECTOR, BENET WEAPONS LABORATORY, ATTN: SMCAR-LCB-TL, OF ANY ADDRESS CHANGES.

TECHNICAL REPORT EXTERNAL DISTRIBUTION LIST

	NO. OF COPIES
ASST SEC OF THE ARMY RESEARCH & DEVELOPMENT ATTN: DEP FOR SCI & TECH THE PENTAGON WASHINGTON, D.C. 20315	1
COMMANDER DEFENSE TECHNICAL INFO CENTER ATTN: DTIC-DDA CAMERON STATION ALEXANDRIA, VA 22314	12
COMMANDER US ARMY MAT DEV & READ COMD ATTN: DRCDE-SG 5001 EISENHOWER AVE ALEXANDRIA, VA 22333	1
COMMANDER ARMAMENT RES & DEV CTR US ARMY AMCCOM ATTN: SMCAR-LC	1
SMCAR-LCE	1
SMCAR-LCM (BLDG 321)	1
SMCAR-LCS	1
SMCAR-LCU	1
SMCAR-LCW	1
SMCAR-SCM-O (PLASTICS TECH EVAL CTR, BLDG. 351N)	1
SMCAR-TSS (STINFO) DOVER, NJ 07801	2
DIRECTOR BALLISTICS RESEARCH LABORATORY ATTN: AMXBR-TSB-S (STINFO) ABERDEEN PROVING GROUND, MD 21005	1
MATERIEL SYSTEMS ANALYSIS ACTV ATTN: DRXSY-MP ABERDEEN PROVING GROUND, MD 21005	1
COMMANDER US ARMY AMCCOM ATTN: SMCAR-ESP-L ROCK ISLAND, IL 61299	1
COMMANDER ROCK ISLAND ARSENAL ATTN: SMCRI-ENM (MAT SCI DIV) ROCK ISLAND, IL 61299	1
DIRECTOR US ARMY INDUSTRIAL BASE ENG ACTV ATTN: DRXIB-M ROCK ISLAND, IL 61299	1
COMMANDER US ARMY TANK-AUTMV R&D COMD ATTN: TECH LIB - DRSTA-TSL WARREN, MI 48090	1
COMMANDER US ARMY TANK-AUTMV COMD ATTN: DRSTA-RC WARREN, MI 48090	1
COMMANDER US MILITARY ACADEMY ATTN: CHMN, MECH ENGR DEPT WEST POINT, NY 10996	1
US ARMY MISSILE COMD REDSTONE SCIENTIFIC INFO CTR ATTN: DOCUMENTS SECT, BLDG. 4484 REDSTONE ARSENAL, AL 35898	2
COMMANDER US ARMY FGN SCIENCE & TECH CTR ATTN: DRXST-SD 220 7TH STREET, N.E. CHARLOTTESVILLE, VA 22901	1

NOTE: PLEASE NOTIFY COMMANDER, ARMAMENT RESEARCH AND DEVELOPMENT CENTER, US ARMY AMCCOM, ATTN: BENET WEAPONS LABORATORY, SMCAR-LCB-TL, WATERVLIET, NY 12189, OF ANY ADDRESS CHANGES.

TECHNICAL REPORT EXTERNAL DISTRIBUTION LIST (CONT'D)

	NO. OF COPIES
COMMANDER US ARMY MATERIALS & MECHANICS RESEARCH CENTER ATTN: TECH LIB - DRXMR-PL WATERTOWN, MA 01272	2
COMMANDER US ARMY RESEARCH OFFICE ATTN: CHIEF, IPO P.O. BOX 12211 RESEARCH TRIANGLE PARK, NC 27709	1
COMMANDER US ARMY HARRY DIAMOND LAB ATTN: TECH LIB 2800 POWDER MILL ROAD ADELPHIA, MD 20783	1
COMMANDER NAVAL SURFACE WEAPONS CTR ATTN: TECHNICAL LIBRARY CODE X212 DAHLGREN, VA 22448	1
DIRECTOR US NAVAL RESEARCH LAB ATTN: DIR, MECH DIV	1
CODE 26-27, (DOC LIB) WASHINGTON, D.C. 20375	1
COMMANDER AIR FORCE ARMAMENT LABORATORY ATTN: AFATL/DLJ	1
AFATL/DLJG EGLIN AFB, FL 32542	1
METALS & CERAMICS INFO CTR BATTELLE COLUMBUS LAB 505 KING AVENUE COLUMBUS, OH 43201	1

NOTE: PLEASE NOTIFY COMMANDER, ARMAMENT RESEARCH AND DEVELOPMENT CENTER, US ARMY AMCCOM, ATTN: BENET WEAPONS LABORATORY, SMCAR-LCB-TL, WATERVLIET, NY 12189, OF ANY ADDRESS CHANGES.